Iranian Journal of Medical Physics

ijmp.mums.ac.ir

Radiation Shielding Features of Ordinary and High-Density Concretes Loaded With PbO Micro and Nanoparticles against High-Energy Photons

Khatibeh Verdipoor [1, 2], Asghar Mesbahi [1, 2*]

1. Molecular Medicine Research Center, Institute of Biomedicine, Tabriz University of Medical Sciences, Tabriz, Iran
2. Medical Radiation Sciences Research Team, Tabriz University of Medical Sciences, Tabriz, Iran

ARTICLE INFO

Article type:
Original Article

Article history:
Received: May 14, 2019
Accepted: Aug 01, 2019

Keywords:
Attenuation Coefficient
Concrete
Nanoparticle
Radiation

ABSTRACT

Introduction: The present study aimed to evaluate the impact of PbO nano and micro-sized fillers on ordinary and heavy concretes for different photon energies.

Material and Methods: The MCNPX Monte Carlo code (version 2.6.0) was used for all simulations in the present study. A model of narrow-beam geometry was validated and utilized to calculate the linear attenuation of samples. Three concentrations of PbO, including the weight of 23%, 37.5%, and 50% were simulated. The nano- and microparticle-loaded concretes were simulated using the Lattice and Universe properties of MCNPX code. Finally, the mass attenuation coefficients of studied concretes were analyzed and compared in this study.

Results: Among all the studied concretes, the highest increase of 11% in attenuation coefficient was seen for concretes doped with PbO nanoparticles. The particle size effect was not observed for 18 MeV photon beam, and maximum difference between nano-fillers and micro-fillers was observed for photon energies around 1 MeV.

Conclusion: The difference between nano-fillers and micro-fillers was not significant for heavy concretes in comparison to that for ordinary concrete. It is recommended to apply PbO nanoparticles as effective filler in the ordinary concrete composition for providing higher shielding performance.

► *Please cite this article as:*

Verdipoor Kh, Mesbahi A. Radiation Shielding Features of Ordinary and High-Density Concretes Loaded With PbO Micro and Nanoparticles against High-Energy Photons. Iran J Med Phys 2020; 17: 205-212. 10.22038/ijmp.2019.40381.1556.

Introduction

Currently, there has been an increase in the application of nanoparticles in the fabrication of new shielding materials [1-4]. In fact, the main reason for using nanoparticles originates from their higher attenuation effect, compared to that of larger particle sizes. Basically, this superiority stems solely from the higher surface to the volume ratio of nanoparticles relative to microparticles utilized in the structure of shielding materials used against photons and neutrons [2,3,5].

The concretes are the main construction and shielding materials used in the diagnostic and therapeutic application of radiation in medicine [6-8]. In radiation therapy with high energy photons (i.e., up to 18 MeV), most of the bunkers are made of ordinary concretes with a density of approximately 2.35 g/cm^3, and the wall thickness may be used up to 3 m [9,10]. Therefore, high-density concretes are employed to reduce the wall thickness and provide a larger usable area for routine procedures in the radiation therapy room.

In recent years, several studies, including experimental and Monte Carlo (MC) simulations, have been conducted to investigate the feasibility of adding different nanoparticles to ordinary and heavy concretes [2,6-8,11,12]. In this regard, the findings of an investigation showed better attenuation for ordinary concrete doped with PbO_2 micro and nanoparticles, compared to that for other fillers, such as WO_3 and Fe_2O_3 nanoparticles [2]. Furthermore, the results of a study indicated that adding Wo_3 and Bi_2O_3 nanoparticles improve the attenuation effect of hematite-serpentine concrete against gamma radiations within the energy range of 142-1330 KeV [13].

Moreover, a recent study carried out by Abo-El-Enein et al. examined the impact of adding Fe_2O_3 and ZnO nanoparticles to Portland cement paste [14]. They reported considerable shielding enhancement of modified paste using hematite nanoparticles. In another study conducted by Hassan et al. (2015), they added PbO and $PbTiO_3$ nanopowders to ordinary

*Corresponding Author: Tel: +98-09141193747; E-mail: amesbahi2010@gmail.com

concrete and observed a considerable attenuation improvement [15].

To the best of our knowledge, there has been no study on doping different high-density concretes with PbO nanoparticles. In addition, it is important to quantitatively compare the PbO filler effect on ordinary- and high-density concretes in a wide range of photon energy used in radiation therapy facilities. Therefore, the present study, investigated the shielding effect of adding PbO micro and nanoparticles to ordinary- and several high-density concretes. Two different particle sizes and three concentrations of PbO particles were studied for detailed comparison.

Materials and Methods

Monte Carlo Simulations

For all MC simulations, the MCNPX (version 2.6.0) MC code was used to calculate the mass attenuation coefficients of all the studied concretes. Micro and nanoparticles were simulated as spheres suspended inside the matrix filled with concretes. In this geometry, the distribution of spherical fillers in concrete matrix was completely homogenous. Microspheres and nanoparticles with diameters of 10 µm and 100 nm were simulated, respectively. Selection of particle size was based on the results of previous studies and with the intention to a better differentiation of filler size effect [11, 13].

A superficial photon source with a radius of 3 mm was used, and the lead collimators with a radius of 20 cm and length of 10 cm were employed to absorb all scattered radiations from the shielding material. In the present study, the schematic representation of geometry is depicted in Figure 1. The collimators provided the conditions of narrow-beam geometry for attenuation calculations. A distance of 100 cm between the source and detector cell was considered in this study. The F4 tally was used for scoring the flux photons reaching the detector cell. This tally calculates the particle flux in terms of particles per cm^2.

One ordinary concrete and four high-density concretes were studied in this study, and their material composition was considered in the simulations. The concrete matrix was filled with PbO fillers in two sizes and various concentrations (See Table 1).

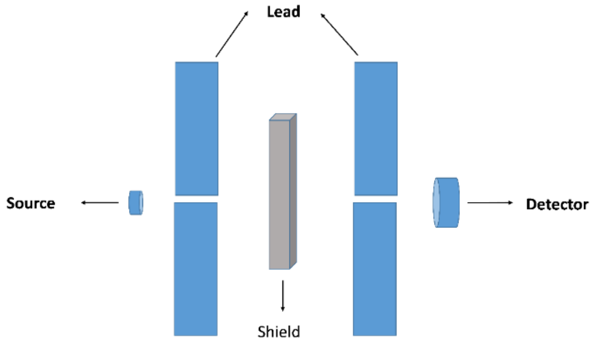

Figure 1. Schematic representation of the designed geometry in MCNPX code

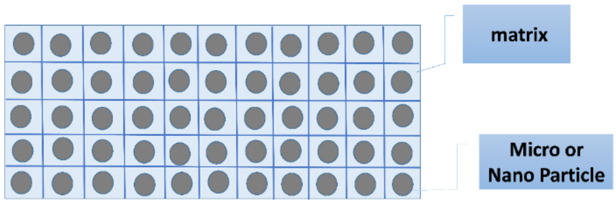

Figure 2. Geometry definition using lattice card in MCNPX code for micro-fillers and nanofillers in concrete matrix

Several concentrations of PbO, including the weight of 23%, 37.5%, and 50% were simulated. Several photon beams, including mono-energetic beams from different radioactive materials, were identified as 0.3559, 0.6638, 0.7786, 0.964, 1.17, 1.33, and 1.407 MeV in a laboratory. Moreover, two poly-energetic photon beams of a conventional Varian linac (2100 CD) 6 and 18 MeV were simulated as photon sources. Photon spectra of published previous studies were used in the photon source definition of MC model [8, 9].

Table 1. Elemental composition of the studied concretes

Concrete type	Density ($g\ cm^{-3}$)	Elemental composite
Ordinary	2.26	H (0.0092) O (0.4983) Na (0.0171) Al (0.0456) Si (0.3158) K (0.0192) Ca (0.0826) Fe (0.0122)
Basalt-Magnetite	3.05	H (0.0083) O (0.423) Na (0.0106) Al (0.0422) Si (0.132) K (0.0029) Ca (0.0888) Fe (0.2601) Ti (0.006) Mn (0.0012) S (0.0009) P (0.002) Mg (0.022)
Barite	3.35	H (0.0036) O (0.3118) Mg (0.0011) Al (0.0042) Si (0.0104) Ca (0.0502) Ba (0.4634) Fe (0.0475) S (0.1078)
Steel scrap	4	H (0.007) C (0.0009) O (0.2109) Na (0.0045) Mg (0.0009) Al (0.012) Si (0.1049) S (0.0006) K (0.003) Ca (0.0428) Fe (0.6125)
Steel-Magnetite	5.11	H (0.0051) O (0.157) Mg (0.0065) Al (0.0066) Si (0.0268) P (0.0008) S (0.0006) Ca (0.0395) Fe (0.7571)

The Lattice and Universe cards of MCNPX code were utilized to simulate micro and nanoparticles (Figure 2). The photon transmission for a thickness of 10-200 cm with an interval of 20 cm was calculated. Then, the curve of transmission against thickness was obtained, and the attenuation coefficient of each sample was derived according to the following formula:

$$I = I_0 \, e^{-\mu x} \qquad (1)$$

Where I and I_0 denote the number of counted photons with and without the presence of concrete, respectively. Mass attenuation coefficients of all the studied samples were calculated by dividing the linear attenuation coefficient by density of the samples.

Results

Figure 3 shows the comparison of the mass attenuation coefficient for lead calculated by the present MC model and data provided by national institute of standards and technology (NIST). This was the benchmark calculation to confirm the accuracy of the present MC model and validate the next MC calculations. The difference lower than 2% was observed between the two datasets, and the MC model was validated in this regard.

Figure 4 depicts the comparison of mass attenuation coefficient for the ordinary concrete doped with micro and nanoparticles with a concentration of 37.5 weight percentage (wt%) at different photon energies. For all the energies, the mass attenuation coefficient of nanoparticle doped concrete was slightly (i.e., about 6%) higher than that of microparticles. Table 2 tabulates the detailed dataset for all the concentrations and energies.

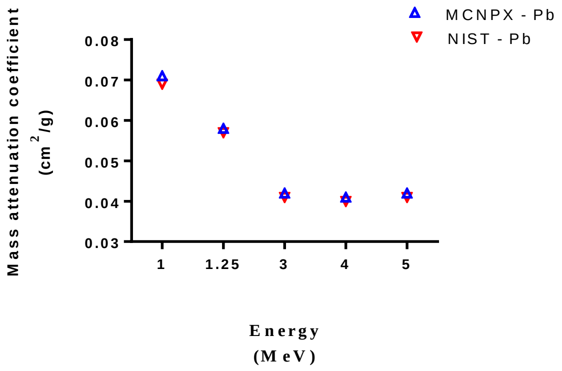

Figure 3. Validation of MCNPX results with national institute of standards and technology reported values for mass attenuation coefficient (cm^2/gr) of lead with different photon energy (MeV)

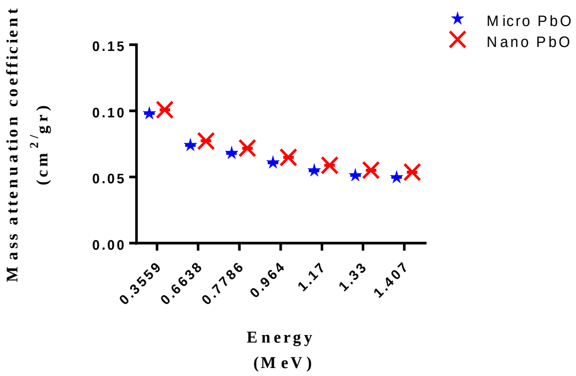

Figure 4. Mass attenuation coefficient (cm^2/g) of ordinary concrete containing 37.5 weight percentage micro and nano of PbO in terms of energy increase

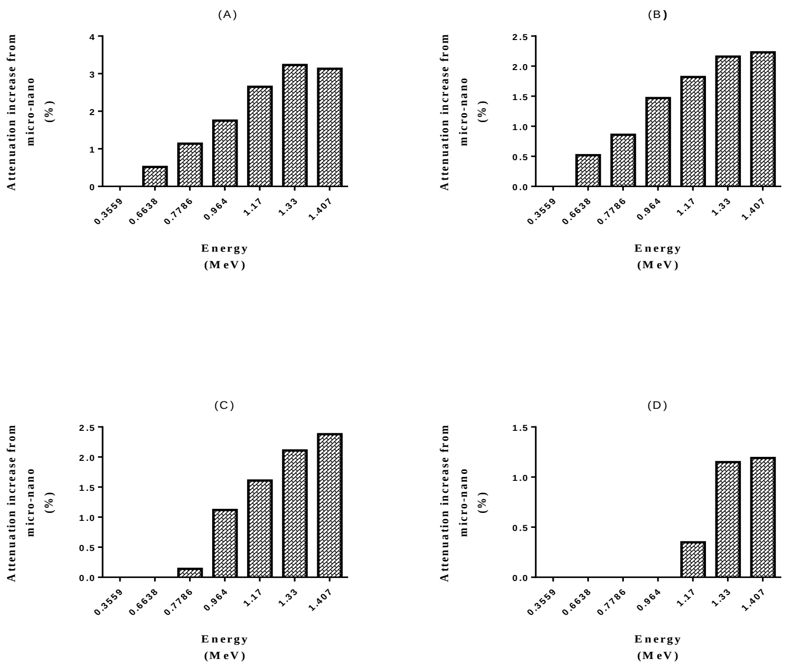

Figure 5. Comparison of attenuation enhancement from micro to nano (%) for heavy-weight concretes containing 23 weight percentage micro and nano of PbO in terms of energy; (A) basalt- magnetite concrete; (B) barite concrete; (C) steel scrap concrete; (D) steel-magnetite concrete

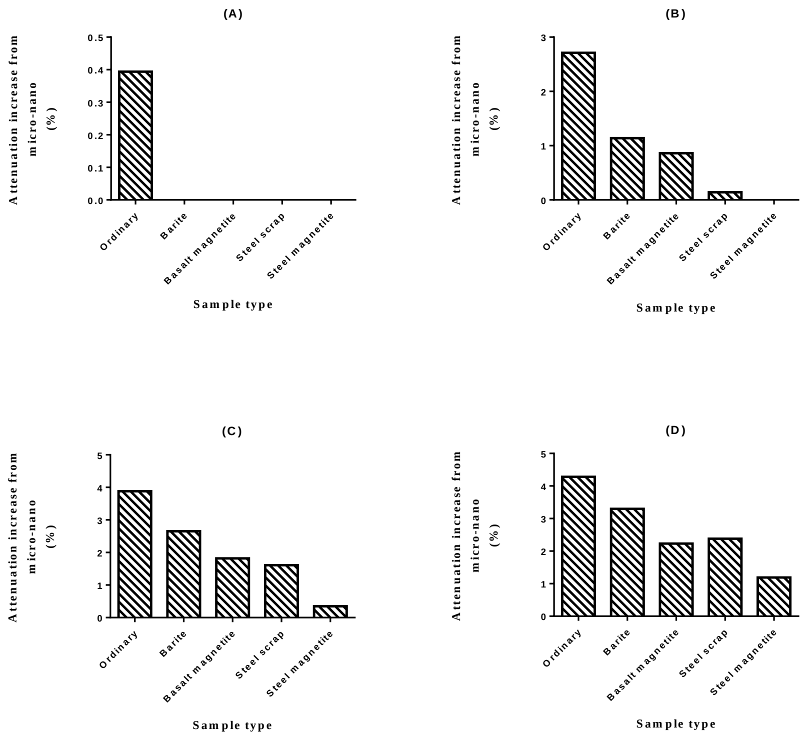

Figure 6. Comparison of attenuation enhancement from micro to nano for heavy concretes containing 23 weight percentage micro and nano of PbO at different photon energies; (A) 0.3559 MeV; (B) 0.7786 MeV; (C) 1.17 MeV; (D) 1.407 MeV

Table 2. Comparison of mass attenuation coefficients (cm^2/gr) of ordinary concrete containing micro and nano PbO at different photon energies (MeV)

Source	Energy (MeV)	Samples	ρ/μ (cm^2/g) Micro	ρ/μ (cm^2/g) Nano	Diff %
Ba^{133}	0.3559	23 wt% PbO and 77 wt% ordinary concrete	0.1013	0.1017	0.394
		37.5 wt% PbO and 62.5 wt% ordinary concrete	0.0981	0.1009	2.85
		50 wt% PbO and 50 wt% ordinary concrete	0.0956	0.1011	5.75
Cs^{137}	0.6638	23 wt% PbO and 77 wt% ordinary concrete	0.0759	0.0773	1.84
		37.5 wt% PbO and 62.5 wt% ordinary concrete	0.074	0.0773	4.45
		50 wt% PbO and 50 wt% ordinary concrete	0.0726	0.0776	6.88
Eu^{152}	0.7786	23 wt% PbO and 77 wt% ordinary concrete	0.0701	0.072	2.71
		37.5 wt% PbO and 62.5 wt% ordinary concrete	0.0681	0.0719	5.58
		50 wt% PbO and 50 wt% ordinary concrete	0.0668	0.0721	7.93
Eu^{152}	0.964	23 wt% PbO and 77 wt% ordinary concrete	0.0628	0.0649	3.34
		37.5 wt% PbO and 62.5 wt% ordinary concrete	0.0609	0.0649	6.56
		50 wt% PbO and 50 wt% ordinary concrete	0.0595	0.0651	9.41
Co^{60}	1.17	23 wt% PbO and 77 wt% ordinary concrete	0.0567	0.0582	3.88
		37.5 wt% PbO and 62.5 wt% ordinary concrete	0.0549	0.0589	7.28
		50 wt% PbO and 50 wt% ordinary concrete	0.0536	0.059	10.07
Co^{60}	1.33	23 wt% PbO and 77 wt% ordinary concrete	0.0527	0.0552	4.74
		37.5 wt% PbO and 62.5 wt% ordinary concrete	0.0513	0.0552	7.6
		50 wt% PbO and 50 wt% ordinary concrete	0.05	0.0553	10.6
Eu^{152}	1.407	23 wt% PbO and 77 wt% ordinary concrete	0.0514	0.0536	4.28
		37.5 wt% PbO and 62.5 wt% ordinary concrete	0.0498	0.0537	7.83
		50 wt% PbO and 50 wt% ordinary concrete	0.0485	0.0536	10.51
Linac photon spectrum	6	23 wt% PbO and 77 wt% ordinary concrete	0.0546	0.0562	2.93
		37.5 wt% PbO and 62.5 wt% ordinary concrete	0.0535	0.0565	5.6
		50 wt% PbO and 50 wt% ordinary concrete	0.052	0.0567	9.03
Linac photon spectrum	18	23 wt% PbO and 77 wt% ordinary concrete	0.0373	0.037	------
		37.5 wt% PbO and 62.5 wt% ordinary concrete	0.0372	0.0371	------
		50 wt% PbO and 50 wt% ordinary concrete	0.0374	0.037	------

wt%: Weight percentage

Table 3. Comparison of mass attenuation coefficients (cm^2/gr) of basalt-magnetite concrete containing micro and nano PbO at different photon energies (MeV)

Source	Energy (MeV)	Samples	ρ/μ (cm^2/g) Micro	ρ/μ (cm^2/g) Nano	%	Diff
		23 wt% PbO and 77 wt% basalt-magnetite concrete	0.1022	0.1008	------	
Ba^{133}	0.3559	37.5 wt% PbO and 62.5 wt% basalt-magnetite concrete	0.1001	0.1007	0.59	
		50 wt% PbO and 50 wt% basalt-magnetite concrete	0.097	0.1008	2.12	
		23 wt% PbO and 77 wt% basalt-magnetite concrete	0.0759	0.0763	0.52	
Cs^{137}	0.6638	37.5 wt% PbO and 62.5 wt% basalt-magnetite concrete	0.0748	0.0763	2	
		50 wt% PbO and 50 wt% basalt-magnetite concrete	0.0739	0.0763	3.24	
		23 wt% PbO and 77 wt% basalt-magnetite concrete	0.0701	0.0709	1.14	
Eu^{152}	0.7786	37.5 wt% PbO and 62.5 wt% basalt-magnetite concrete	0.0686	0.0709	3.35	
		50 wt% PbO and 50 wt% basalt-magnetite concrete	0.0678	0.0711	4.86	
		23 wt% PbO and 77 wt% basalt-magnetite concrete	0.0626	0.0637	1.75	
Eu^{152}	0.964	37.5 wt% PbO and 62.5 wt% basalt-magnetite concrete	0.0611	0.064		4.74
		50 wt% PbO and 50 wt% basalt-magnetite concrete	0.0603	0.0639	5.97	
		23 wt% PbO and 77 wt% basalt-magnetite concrete	0.0564	0.0579	2.65	
Co^{60}	1.17	37.5 wt% PbO and 62.5 wt% basalt-magnetite concrete	0.0549	0.058		5.63
		50 wt% PbO and 50 wt% basalt-magnetite concrete	0.054	0.058	7.4	
		23 wt% PbO and 77 wt% basalt-magnetite concrete	0.0525	0.0542	3.23	
Co^{60}	1.33	37.5 wt% PbO and 62.5 wt% basalt-magnetite concrete	0.0511	0.0543		6.26
		50 wt% PbO and 50 wt% basalt-magnetite concrete	0.0501	0.0542	8.18	
		23 wt% PbO and 77 wt% basalt-magnetite concrete	0.0511	0.0527	3.13	
Eu^{152}	1.407	37.5 wt% PbO and 62.5 wt% basalt-magnetite concrete	0.0496	0.0528	6.45	
		50 wt% PbO 50 wt% basalt-magnetite concrete	0.0486	0.0528	8.64	
Linac		23 wt% PbO and 77 wt% basalt-magnetite concrete	0.054	0.0549	1.67	
photon	6	37.5 wt% PbO and 62.5 wt% basalt-magnetite concrete	0.053	0.055	3.77	
spectrum		50 wt% PbO and 50 wt% basalt-magnetite concrete	0.0519	0.0552	6.35	
Linac		23 wt% PbO and 77 wt% basalt-magnetite concrete	0.0375	0.0369	------	
photon	18	37.5 wt% PbO and 62.5 wt% basalt-magnetite concrete	0.0378	0.037	------	
spectrum		50 wt% PbO and 50 wt% basalt-magnetite concrete	0.0377	0.0371	------	

wt%: Weight percentage

Table 4. Comparison of mass attenuation coefficients (cm^2/gr) of barite concrete containing micro and nano PbO at different photon energies (MeV).

Source	Energy (MeV)	Samples	ρ/μ (cm^2/g) Micro	ρ/μ (cm^2/g) Nano	%	Diff
		23 wt% PbO and 76 wt% barite concrete	0.1012	0.1008	------	
Ba^{133}	0.3559	37.5 wt% PbO and 62.5 wt% barite concrete	0.1011	0.1008	------	
		50 wt% PbO and 50 wt% barite concrete	0.1001	0.1005	0.69	
		23 wt% PbO and 76 wt% barite concrete	0.0763	0.0767	0.52	
Cs^{137}	0.6638	37.5 wt% PbO and 62.5 wt% barite concrete	0.0761	0.0768	0.91	
		50 wt% PbO and 50 wt% barite concrete	0.0755	0.0768	1.72	
		23 wt% PbO and 76 wt% barite concrete	0.0695	0.0701	0.86	
Eu^{152}	0.7786	37.5 wt% PbO and 62.5 wt% barite concrete	0.069	0.0701	1.59	
		50 wt% PbO and 50 wt% barite concrete	0.0683	0.0701	2.63	
		23 wt% PbO and 76 wt% barite concrete	0.0612	0.0621	1.47	
Eu^{152}	0.964	37.5 wt% PbO and 62.5 wt% barite concrete	0.0607	0.0622	2.47	
		50 wt% PbO and 50 wt% barite concrete	0.0601	0.0622	3.66	
		23 wt% PbO and 76 wt% barite concrete	0.0547	0.0557	1.82	
Co^{60}	1.17	37.5 wt% PbO and 62.5 wt% barite concrete	0.0542	0.0557		2.76
		50 wt% PbO and 50 wt% barite concrete	0.0534	0.0559	4.68	
		23 wt% PbO and 76 wt% barite concrete	0.0508	0.0519	2.16	
Co^{60}	1.33	37.5 wt% PbO and 62.5 wt% barite concrete	0.0503	0.052	3.37	
		50 wt% PbO and 50 wt% barite concrete	0.0495	0.0521	5.89	
		23 wt% PbO and 76 wt% barite concrete	0.0492	0.0503	2.23	
Eu^{152}	1.407	37.5 wt% PbO and 62.5 wt% barite concrete	0.0488	0.0505	3.48	
		50 wt% PbO and 50 wt% barite concrete	0.0479	0.0503	5.01	
Linac		23 wt% PbO and 76 wt% barite concrete	0.0545	0.0555	1.83	
photon	6	37.5 wt% PbO and 62.5 wt% barite concrete	0.0535	0.0554		3.55
spectrum		50 wt% PbO and 50 wt% barite concrete	0.0535	0.056	4.67	
Linac		23 wt% PbO and 76 wt% barite concrete	0.0389	0.0387	------	
photon	18	37.5 wt% PbO and 62.5 wt% barite concrete	0.0391	0.0387		------
spectrum		50 wt% PbO and 50 wt% barite concrete	0.0-39	0.0387	------	

wt%: Weight percentage

Table 5. Comparison of mass attenuation coefficients (cm^2/gr) of steel scrap concrete containing micro and nano PbO at different photon energies (MeV)

Source	Energy (MeV)	Samples	μ/ρ (cm^2/g) Micro	μ/ρ (cm^2/g) Nano	Diff %
Ba^{133}	0.3559	23 wt% PbO and 77 wt% steel scrap concrete	0.1032	0.1007	------
		37.5 wt% PbO and 62.5 wt% steel scrap concrete	0.103	0.1005	------
		50 wt% PbO and 50 wt% steel scrap concrete	0.1036	0.1006	------
Cs^{137}	0.6638	23 wt% PbO and 77 wt% steel scrap concrete	0.0756	0.075	------
		37.5 wt% PbO and 62.5 wt% steel scrap concrete	0.0754	0.0751	------
		50 wt% PbO and 50 wt% steel scrap concrete	0.0764	0.0749	------
Eu^{152}	0.7786	23 wt% PbO and 77 wt% steel scrap concrete	0.0696	0.0697	0.14
		37.5 wt% PbO and 62.5 wt% steel scrap concrete	0.0691	0.0696	0.72
		50 wt% PbO and 50 wt% steel scrap concrete	0.069	0.0697	1.01
Eu^{152}	0.964	23 wt% PbO and 77 wt% steel scrap concrete	0.062	0.0627	1.12
		37.5 wt% PbO and 62.5 wt% steel scrap concrete	0.0614	0.0627	2.11
		50 wt% PbO and 50 wt% steel scrap concrete	0.0613	0.0627	2.28
Co^{60}	1.17	23 wt% PbO and 77 wt% steel scrap concrete	0.0558	0.0567	1.61
		37.5 wt% PbO and 62.5 wt% steel scrap concrete	0.055	0.0567	3.09
		50 wt% PbO and 50 wt% steel scrap concrete	0.0547	0.0567	3.65
Co^{60}	1.33	23 wt% PbO and 77 wt% steel scrap concrete	0.0519	0.053	2.11
		37.5 wt% PbO and 62.5 wt% steel scrap concrete	0.0513	0.0532	4.53
		50 wt% PbO and 50 wt% steel scrap concrete	0.0507	0.053	4.53
Eu^{152}	1.407	23 wt% PbO and 77 wt% steel scrap concrete	0.0504	0.0516	2.38
		37.5 wt% PbO and 62.5 wt% steel scrap concrete	0.0498	0.0517	3.81
		50 wt% PbO and 50 wt% steel scrap concrete	0.0493	0.0516	4.66
Linac photon spectrum	6	23 wt% PbO and 77 wt% steel scrap concrete	0.0529	0.0525	1.34
		37.5 wt% PbO and 62.5 wt% steel scrap concrete	0.0522	0.0534	2.29
		50 wt% PbO and 50 wt% steel scrap concrete	0.052	0.0534	2.69
Linac photon spectrum	18	23 wt% PbO and 77 wt% steel scrap concrete	0.0379	0.0372	------
		37.5 wt% PbO and 62.5 wt% steel scrap concrete	0.0381	0.0373	------
		50 wt% PbO and 50 wt% steel scrap concrete	0.0386	0.0373	------

wt%: Weight percentage

Table 6. Comparison of mass attenuation coefficients (cm^2/gr) of steel-magnetite concrete containing micro and nano PbO at different photon energies (MeV)

Source	Energy (MeV)	Samples	μ/ρ (cm^2/g) Micro	μ/ρ (cm^2/g) Nano	Diff %
Ba^{133}	0.3559	23 wt% PbO and 76 wt% steel-magnetite concrete	0.1053	0.1004	------
		37.5 wt% PbO and 62.5 wt% steel-magnetite concrete	0.1072	0.1006	------
		50 wt% PbO and 50 wt% steel-magnetite concrete	0.1093	0.1003	------
Cs^{137}	0.6638	23 wt% PbO and 76 wt% steel-magnetite concrete	0.0763	0.0744	------
		37.5 wt% PbO and 62.5 wt% steel-magnetite concrete	0.0771	0.0744	------
		50 wt% PbO and 50 wt% steel-magnetite concrete	0.0787	0.0744	------
Eu^{152}	0.7786	23 wt% PbO and 76 wt% steel-magnetite concrete	0.0701	0.0689	------
		37.5 wt% PbO and 62.5 wt% steel-magnetite concrete	0.0704	0.0689	------
		50 wt% PbO and 50 wt% steel-magnetite concrete	0.0712	0.069	------
Eu^{152}	0.964	23 wt% PbO and 76 wt% steel-magnetite concrete	0.0624	0.062	------
		37.5 wt% PbO and 62.5 wt% steel-magnetite concrete	0.0623	0.0621	------
		50 wt% PbO and 50 wt% steel-magnetite concrete	0.0625	0.0621	------
Co^{60}	1.17	23 wt% PbO and 76 wt% steel-magnetite concrete	0.0559	0.0561	0.35
		37.5 wt% PbO and 62.5 wt% steel-magnetite concrete	0.0555	0.056	0.9
		50 wt% PbO and 50 wt% steel-magnetite concrete	0.0555	0.0561	1.08
Co^{60}	1.33	23 wt% PbO and 76 wt% steel-magnetite concrete	0.0519	0.0525	1.15
		37.5 wt% PbO and 62.5 wt% steel-magnetite concrete	0.0515	0.0525	1.94
		50 wt% PbO and 50 wt% steel-magnetite concrete	0.0515	0.0525	1.94
Eu^{152}	1.407	23 wt% PbO and 76 wt% steel-magnetite concrete	0.0504	0.051	1.19
		37.5 wt% PbO and 62.5 wt% steel-magnetite concrete	0.05	0.0511	2.2
		50 wt% PbO and 50 wt% steel-magnetite concrete	0.0499	0.0511	2.4
Linac photon spectrum	6	23 wt% PbO and 76 wt% steel-magnetite concrete	0.0522	0.0524	0.38
		37.5 wt% PbO and 62.5 wt% steel-magnetite concrete	0.052	0.0524	0.76
		50 wt% PbO and 50 wt% steel-magnetite concrete	0.052	0.0525	0.94
Linac photon spectrum	18	23 wt% PbO and 76 wt% steel-magnetite concrete	0.038	0.037	------
		37.5 wt% PbO and 62.5 wt% steel-magnetite concrete	0.0386	0.037	------
		50 wt% PbO and 50 wt% steel-magnetite concrete	0.0387	0.037	------

wt%: Weight percentage

Figure 7 depicts the attenuation increase for nanoparticle filler, compared to that of microparticles for energy spectrum of 6MV photon beam. In a similar pattern to mono-energetic beams, the highest increase occurred for the ordinary concrete, and among high-density concretes the maximum gain was obtained for basalt-magnetite and barite concretes. Tables 2-6 tabulate the mass attenuation coefficient for studied concretes in terms of photon energy, filler concentration, and particle size.

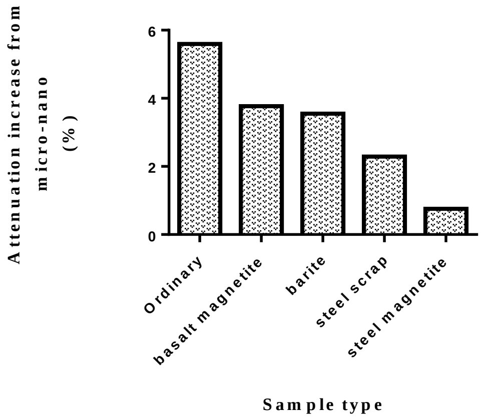

Figure 7. Comparison of attenuation increase from micro to nano for heavy concretes containing 23 weight percentage micro and nano of PbO at photon energy of 6 MeV

Discussion

As it is shown in tables 2-6, the mass attenuation coefficient decreases with photon energy, and the lowest value is observed for poly-energetic 18 MeV photon beam of the medical linac. The difference between micro-fillers and nano-fillers gradually increased with photon energy, and the maximum difference of 10.6% was reported for the ordinary concrete for the concentration of 50 wt% (See Table 2). Effect of particle size was not observed in the 18 MeV photon beam for all the concretes and concentrations. However, for the 6 MeV photon beam, the filler size effect existed for the ordinary, basalt-magnetite, and barite concretes.

Results of the present study can be compared with those of an experimental study performed by Hassan et al. (2015) who added PbO nano-powders to ordinary concrete [15]. In the concentration of 50 wt% for 667, 1173, and 1332 keV photons, a close agreement (i.e., 0.057 vs. 0.055 µm) was observed between the present MC and their measurement results. The PbO_2, PbO, and $PbTiO_3$ fillers were added in the aforementioned study. In addition, the highest mass attenuation coefficient was reported for PbO fillers.

Furthermore, in a similar MC study carried out by Tekin et al., the hematite-serpentine concrete was doped with WO_3 and Bi_2O_3 micro and nanoparticles [13]. They showed approximately 6.5-7.7% and 5.7-7% increase in mass attenuation coefficient for WO_3 and Bi_2O_3 nanoparticles respectively within the photon energy range of 142-1330 keV. Composition of the studied concretes in the present study differed from that of the aforementioned studied concretes; therefore, exact comparison cannot be made between the two studies. Nonetheless, the results of the present study for basalt-magnetite concrete at the concentration of 50 wt% are close to the reported values of the aforementioned study in terms of the mass attenuation coefficient for ^{60}Co gamma rays. In addition, a similar enhancement of mass attenuation coefficient for nanofiller compared to micro-filler was found for the current study and Tekin et al results. The small differences between the results of the present study and the findings of the two abovementioned studies can be due to the differences in nano and microparticles sizes, as well as concrete compositions. However, it should be noted that the present study considered higher photon energies, including the photon spectra of 6 and 18 MeV beams of a medical linac, which provided more data for the application of these concretes in radiation therapy facilities.

Finding of the present study on the ordinary concrete doped with PbO (i.e., 50 wt%) can be compared with the results of a recent study by Mesbahi et al. that added PbO_2 to ordinary concrete. However, the values of the aforementioned study for mass attenuation coefficients (i.e., 0.076 at the energy of 1250 keV) were slightly higher than those of the present study. It can be attributed to the small difference in nanoparticles atomic composition, as well as smaller size of PbO_2 nanoparticles (i.e, 50 nm) in the above-mentioned study [2].

Conclusion

The present study evaluated the effect of adding PbO filler in two sizes, including micro and nanometers to one ordinary and four heavy concretes. According to the obtained results, it can be concluded that the attenuation properties of all the concretes enhanced with the filler concentration for all the studied photon energies. Moreover, the effect of filler size was dependent on photon energy and concrete type. The highest increase in attenuation was observed for the ordinary concrete in the photon energy around 1 MeV.

It can be concluded that using nanofillers to increase the attenuation coefficient of heavy concrete is not advantageous relative to microparticles. Moreover, the superiority of nanoparticle fillers relative to microparticles diminished at the higher energy of photon (i.e., 18 MeV) used in radiation therapy facilities. Finally, it is strongly recommended to apply both PbO micro and nanoparticles as effective additives in the composition of ordinary concrete to enhance its shielding property.

Acknowledgment

The authors would like to thank Molecular Medicine Research Center and Medical Radiation Sciences Research Team of Tabriz University of Medical Sciences, Tabriz, Iran, for providing required computational facilities.

References

1. Li R, Gu Y, Wang Y, Yang Z, Li M, Zhang Z Effect of particle size on gamma radiation shielding property of gadolinium oxide dispersed epoxy resin matrix composite. Materials Research Express. 2017;4: 35-8.
2. Mesbahi A, Ghiasi H. Shielding properties of the ordinary concrete loaded with micro- and nano-particles against neutron and gamma radiations. Applied Radiation and Isotopes. 2018;136:27-31.
3. Nambiar S, Yeow JTW. Polymer-composite materials for radiation protection. ACS Applied Materials and Interfaces. 2012;4:5717-26.
4. Noor Azman NZ, Siddiqui SA, Hart R, Low IM. Effect of particle size, filler loadings and x-ray tube voltage on the transmitted x-ray transmission in tungsten oxide-epoxy composites. Applied Radiation and Isotopes. 2013;71:62-7.
5. Tekin HO, Sayyed MI, Altunsoy EE, Manici T. Shielding properties and effects of WO3 and PbO on mass attenuation coefficients by using MCNPX code. Digest Journal of Nanomaterials and Biostructures. 2017;12:861-7.
6. Mesbahi A, Ghiasi H, Rabee Mahdavi S. Photoneutron and capture gamma dose calculations for a radiotherapy room made of high density concrete. Nuclear Technology and Radiation Protection. 2011;26:147-52.
7. Mesbahi A, Alizadeh G, Seyed-Oskoee G, Azarpeyvand AA. A new barite-colemanite concrete with lower neutron production in radiation therapy bunkers. Annals of Nuclear Energy. 2013;51:107-11.
8. Mesbahi A, Khaldari R. Neutron and photon scattering properties of high density concretes used in radiation therapy facilities: A Monte Carlo study. Polish Journal of Medical Physics and Engineering. 2017;23:61-5.
9. Khaldari R, Mesbahi A, Kara U. Monte carlo calculation of shielding properties of newly developed heavy concretes for megavoltage photon beam spectra used in radiation therapy. Iranian Journal of Medical Physics. 2016;13:250-60.
10. Mesbahi A, Khaldari R. Monte Carlo calculation of shielding parameters for fast neutrons in newly developed heavy concretes. Iranian Journal of Medical Physics. 2018;15:214.
11. Tekin HO, Singh VP, Manici T. Effects of micro-sized and nano-sized WO3 on mass attenauation coefficients of concrete by using MCNPX code. Applied Radiation and Isotopes. 2017;121:122-5.
12. Verdipoor K, Alemi A, Mesbahi A. Photon mass attenuation coefficients of a silicon resin loaded with WO3, PbO, and Bi2O3 Micro and Nano-particles for radiation shielding. Radiation Physics and Chemistry. 2018;147:85-90.
13. Tekin HO, Sayyed MI, Issa SAM. Gamma radiation shielding properties of the hematite-serpentine concrete blended with WO3 and Bi2O3 micro and nano particles using MCNPX code. Radiation Physics and Chemistry. 2018;150:95-100.
14. Abo-El-Enein SA, El-Hosiny FI, El-Gamal SMA, Amin MS, Ramadan M. Gamma radiation shielding, fire resistance and physicochemical characteristics of Portland cement pastes modified with synthesized Fe2O3 and ZnO nanoparticles. 2018;173:687-706.
15. Hassan HE, Badran HM, Aydarous A, Sharshar T. Studying the effect of nano lead compounds additives on the concrete shielding properties for -rays. Nuclear Instruments and Methods in Physics Research, Section B. Beam Interactions with Materials and Atoms. 2015;360:81-9.